ChemPubSoc Europe

DOI: 10.1002/cplu.201500492

CHEMPLUSCHEM Full Papers

Direct Catalytic Transformation of Biomass Derivatives into Biofuel Component γ-Valerolactone with Magnetic Nickel–Zirconium Nanoparticles

Hu Li,[a, b] Zhen Fang,*[a] and Song Yang[b]

A series of mixed oxide nanoparticles were prepared by a co-precipitation method and characterized by many techniques. Nickel–zirconium oxide catalysts and their partially reduced magnetic counterparts were highly efficient in the direct transformation of biomass derivatives, including ethyl levulinate, fructose, glucose, cellobiose, and carboxymethyl cellulose, into γ-valerolactone (GVL) without the use of an external hydrogen source, producing a maximum GVL yield of 95.2% at 200 °C for 3 h with hydrogen-reduced magnetic Zr_5Ni_5 nanoparticles (< 20 nm). The acid–base bifunctionality of these nanocatalysts plays a synergic role in the synthesis of GVL in alcohols, whereas appropriate control of the nickel/zirconium molar ratio is able to improve the selectivity towards GVL (≈98%), along with high formation rates (up to 54.9 mmol g^{-1} h^{-1}). Moreover, the magnetic Zr_5Ni_5 nanoparticles were conveniently recovered by means of a magnet for five cycles with almost constant activity.

Introduction

Efficient transformations of biomass to produce biofuels and value-added chemicals are deemed as one of promising ways to alleviate the current reliance on fossil fuel sources.[1] In recent years, γ-valerolactone (GVL) has been identified as a green and renewable solvent to improve the performance of biomass conversion and various organic reactions,[2] and as an additive suitable for liquid fuels, perfumes, and food.[3] More importantly, GVL can be employed as a precursor to produce gasoline and diesel fuels (e.g., C_8–C_{18} alkanes and 2-methyltetrahydrofuran) and valuable chemicals, such as 1,4-pentanediol, methyl pentenoate,[4] ionic liquids,[5] and polymers.[6]

Levulinic acid (LA) and its esters, which can be synthesized from lignocellulosic biomass through multiple catalytic steps, are frequently used as substrates for producing GVL with or without enantioselectivity.[7] Among various catalytic processes, noble metals (e.g., gold, platinum, palladium, iridium, and ruthenium particles) show moderate to excellent activity in the catalytic conversion of LA into GVL with hydrogen gas as the hydrogen donor.[8] Metals in the homogeneous phase are active for this catalytic process,[9] although high reaction temperatures (≈200 °C) are normally required to produce GVL with high selectivity from LA in the absence of acid additives over heterogeneous catalysts.[10] In some cases, GVL can be produced at lower temperatures (100 °C), but other parameters, such as high hydrogen partial pressure (e.g., 10 MPa), are required.[11] Interestingly, remarkably enhanced activity in the synthesis of GVL (≈90% yields) from LA at relatively low temperatures can be achieved with strongly acidic cocatalysts (e.g., Amberlyst A15 and A70) or supports, such as DOWEX 50WX2-100, sulfonated polyethersulfone, and acid-functionalized mesoporous carbon, in combination with metal particles, especially ruthenium.[12] It has been speculated that the synergic effect between acids and noble-metal components plays a significant role in facilitating the conversion of LA into GVL through either catalytic hydrogenation of dehydrated products, α- and β-angelica lactones, or intramolecular esterification of in situ generated 4-hydroxypentanoic acid, which is a hydrogenated intermediate.[13] On the other hand, some non-noble-metal catalysts (e.g., nickel, copper, iron, and cobalt) have also been explored in the upgrading of LA to GVL to reduce production costs.[14] Unfortunately, few examples mediated by non-noble-metal catalysts display comparable activities to those of noble metals in the catalytic transformation of LA and its esters into GVL.[15]

Both formic acid (FA) and LA can be obtained from sugars in equal molar ratios, which results in the synthesis of GVL from LA with FA as a hydrogen donor being highly renewable and more attractive. Deng et al. reported that the presence of organic base (e.g., triethylamine and pyridine) could accelerate the decomposition of FA,[16] which was responsible for the enhanced reactivity,[17] but a stronger base (e.g., NaOH and KOH) resulted in decreased GVL yields because of side reactions (e.g., condensation). Recently, a Shvo catalyst was demonstrated to be highly active for producing GVL through solvent-free transfer hydrogenation of LA after reacting at 100 °C for 8 h.[18]

[a] Dr. H. Li, Prof. Z. Fang
Chinese Academy of Sciences, Biomass Group
Key Laboratory of Tropical Plant Resources and Sustainable Use
Xishuangbanna Tropical Botanical Garden
88 Xuefulu, Kunming, Yunnan 650223 (P. R. China)
E-mail: zhenfang@xtbg.ac.cn

[b] Dr. H. Li, Prof. S. Yang
State-Local Joint Engineering Laboratory for Comprehensive Utilization of Biomass, Center for R&D of Fine Chemicals
Guizhou University, Guiyang 550025 (P. R. China)

Supporting information for this article is available on the WWW under http://dx.doi.org/10.1002/cplu.201500492.

Unlike $[RuCl_3]$[16] and $[Ru(acac)_3]$ (acac = acetylacetonate),[4a,9b,c] heterogeneous catalysts, such as silica-immobilized Ru particles, Au/ZrO_2, and Cu/ZrO_2 have recently been investigated for the production of GVL from LA to simplify catalyst recovery.[19] However, only a very limited number of non-noble metals are acid resistant and can selectively catalyze the decomposition of FA into H_2 and CO_2, rather than CO and H_2O.[19c,20]

By using inexpensive and abundant alcohols as hydrogen donors, catalytic transfer hydrogenation (CTH) of LA and its esters to form GVL over non-noble metals and oxides has attracted much attention.[21] Three different reaction routes mediated by acid and/or base sites are generally proposed for the catalytic transformation of ethyl levulinate (EL) into GVL: 1) Lewis acids are able to initially catalyze the hydrogenation of levulinates into 4-hydroxypentanoates, followed by lactonization, to yield GVL.[22] 2) In a basic alcoholic solution with metal particles, GVL is most likely to be produced through the cyclization of LA to form the hydroxy lactone, followed by hydrogen transfer reduction of α-angelica lactone, which is a dehydration product of hydroxy lactone.[23] 3) Basic sites (O^{2-}), with the aid of Lewis acidic sites, have recently been proposed to synergistically activate the dissociation of hydroxyl groups in alcohols for CTH reaction to give 4-hydroxypentanoate, which is subjected to intramolecular esterification or transesterification to produce GVL.[24] Nevertheless, the one-pot transformation of more accessible biomass derivatives, such as sugars, into GVL over a single catalyst is hard to realize because of the need for multiple sequential reaction steps, which involve the formation of hydroxymethylfurfural (HMF), LA, and other intermediates or byproducts,[25] largely restricts its catalytic activity.[26]

Herein, a series of magnetic nickel–zirconium nanoparticles were prepared through a facile and cheap method that involved coprecipitation and partial reduction. These nanoparticles were tested for GVL production and easily separated from the products by means of a magnet. Several important parameters, such as acid–base bifunctionality, nickel/zirconium molar ratio, reaction time, and temperature were optimized to directly convert sugars (e.g., fructose, glucose, cellobiose and carboxymethyl cellulose) and EL into GVL in alcohols without the use of an external hydrogen source.

Results and Discussion

Characterization of catalysts

The XRD patterns of samples of ZrO_2 and NiZr (Ni_2Zr_8, Ni_5Zr_5, and Ni_8Zr_2) are illustrated in Figure 1. Neat ZrO_2 calcined at 450 °C exhibits a series of wide peaks at $2\theta = 30.5$ and 34.6° (tetragonal phase), 28.4 and 31.5° (monoclinic zirconia), and 50.4 and 60.1° (cubic phase). However, only two broad bands, approximately 31.5 and 50.4°, from the characteristic reflections of ZrO_2 are observed in Ni_2Zr_8 and Ni_5Zr_5 oxides; this demonstrates that NiO and ZrO_2 powders primarily exist in noncrystalline phases with small particle sizes. When the molar ratio of Ni/Zr increases to 8:2, a range of additional diffraction peaks at 37.2, 43.3, 62.9, 75.4, and 79.2° are detected, which can be assigned to the reflections of the NiO crystalline structure from the (111), (200), (220), (311), and (222) planes, respectively. Moreover, the actual compositions of NiZr samples determined by inductively coupled plasma optical emission spectroscopy (ICP-OES) are consistent with the controlled Ni/Zr molar ratios (Table 1).

The textural properties of samples of ZrO_2 and NiZr (Ni_2Zr_8, Ni_5Zr_5, and Ni_8Zr_2) were examined by N_2 adsorption–desorption isotherms and pore size distributions (Figure 2 and Figure 1S in the Supporting Information), and results of BET surface areas and average pore sizes of these samples are listed in Table 1. For samples of Ni_2Zr_8 and Ni_5Zr_5, the type IV hysteresis loops of

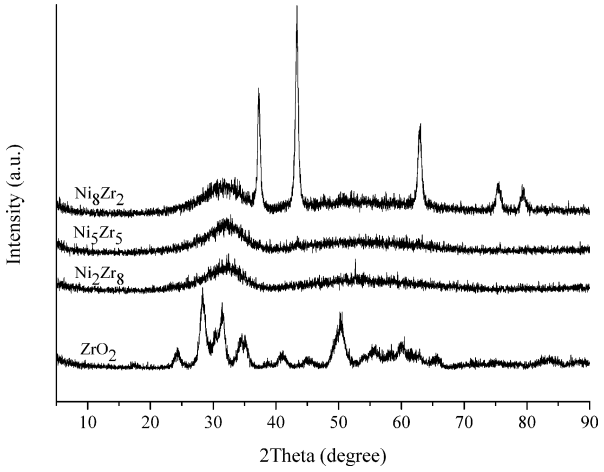

Figure 1. XRD patterns of ZrO_2 and NiZr oxides with different Ni/Zr molar ratios.

Table 1. Physicochemical properties of ZrO_2 and NiZr nanoparticles with different Ni/Zr molar ratios.

Sample	$N_{Ni/Zr}$[a]	BET surface area [$m^2 g^{-1}$]	Pore size [nm][b]	Acidity [$mmol g^{-1}$][c]	Basicity [$mmol g^{-1}$][d]	Ms [$Am^2 kg^{-1}$][e]	Particle size [nm][f]
ZrO_2	–	84.8	7.4	0.35	0.46	–	82.3
Ni_2Zr_8	1:4.18	123.7	5.9	0.59	0.62	2.2	12.5
Ni_5Zr_5	1:1.27	147.2	5.5	0.72	0.53	10.7	19.6
Ni_8Zr_2	3.68:1	91.6	14.1	0.87	0.49	22.6	55.4

[a] The Ni/Zr molar ratio ($N_{Ni/Zr}$) was determined by ICP-OES. [b] Average pore size was calculated by using the Barrett–Joyner–Halenda (BJH) method. [c] Determined by NH_3 temperature-programmed desorption (TPD). [d] Determined by CO_2-TPD. [e] Saturation magnetization (Ms) was determined from the corresponding H_2-reduced NiZr oxides. [f] The crystallite sizes of ZrO_2 and H_2-reduced NiZr samples were estimated from TEM images.

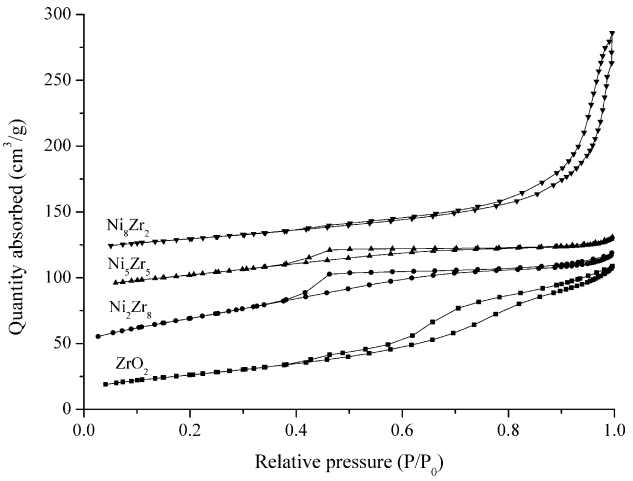

Figure 2. BET analyses of ZrO_2 and NiZr oxides with different Ni/Zr molar ratios.

isotherms suggest the presence of mesoporous structures. With respect to the sample of Ni_8Zr_2, the relative pressure of the loop significantly shifted to 0.8–1.0, which was concomitant with the decreased BET surface area, but increased average pore size, compared with ZrO_2, Ni_2Zr_8, and Ni_5Zr_5 (Table 1). Furthermore, the acid/base strength and contents of the ZrO_2 and NiZr samples were measured by CO_2-/NH_3-TPD, respectively (Figures 2S and 3S, respectively, in the Supporting Information). Two CO_2 desorption bands at approximately 150 and 450 °C for all tested samples are observed (Figure 2S in the Supporting Information) from the weak and moderate base strengths, respectively. Interestingly, the base density is closely correlated with ZrO_2 content and surface area (Table 1). On the other hand, the temperature for NH_3 desorption gradually shifts from approximately 130 to 150 °C, related to weak acidity, as the molar ratio of Ni/Zr increases from 0 to 8:2 (Figure 3S in the Supporting Information).

Saturation magnetization (Ms) of H_2-reduced NiZr samples was also investigated by vibrating sample magnetometry (VSM; Figure 3). With increase Ni species content, the Ms for

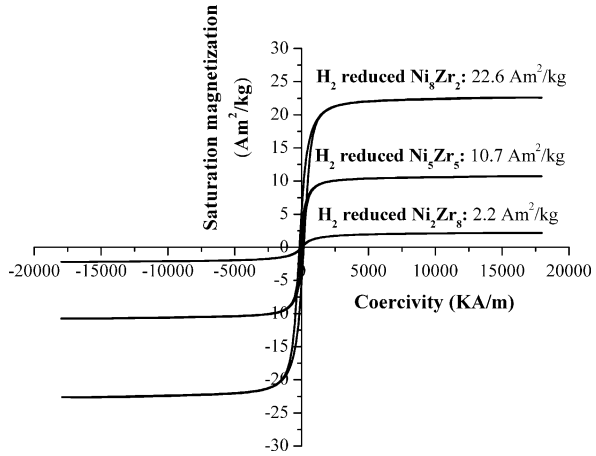

Figure 3. VSM curves of H_2-reduced NiZr catalysts with different Ni/Zr molar ratios.

H_2-reduced Ni_2Zr_8, Ni_5Zr_5, and Ni_8Zr_2 correspondingly increased and was 2.2, 10.7, and 22.6 Am^2kg^{-1}, respectively (Table 1); this means the resulting magnetic materials can be separated from solution with a magnet (Figure 4S in the Supporting Information). The presence of Ni^0 species in reduced NiZr samples can be confirmed by X-ray photoelectron spectroscopy (XPS) with a binding energy of 852.8 eV (Figures 5S and 6S in the Supporting Information). All reduced NiZr samples are nanosized particles (Table 1), which can be estimated from a TEM image by taking Ni_2Zr_8, for example (Figure 4a). In addition, the HRTEM (high-resolution TEM) image of H_2-reduced Ni_2Zr_8 nanoparticles shows a series of typical lattice planes for NiO and ZrO_2 species (Figure 4b), which are consistent with the XRD pattern (Figure 7S in the Supporting Information).

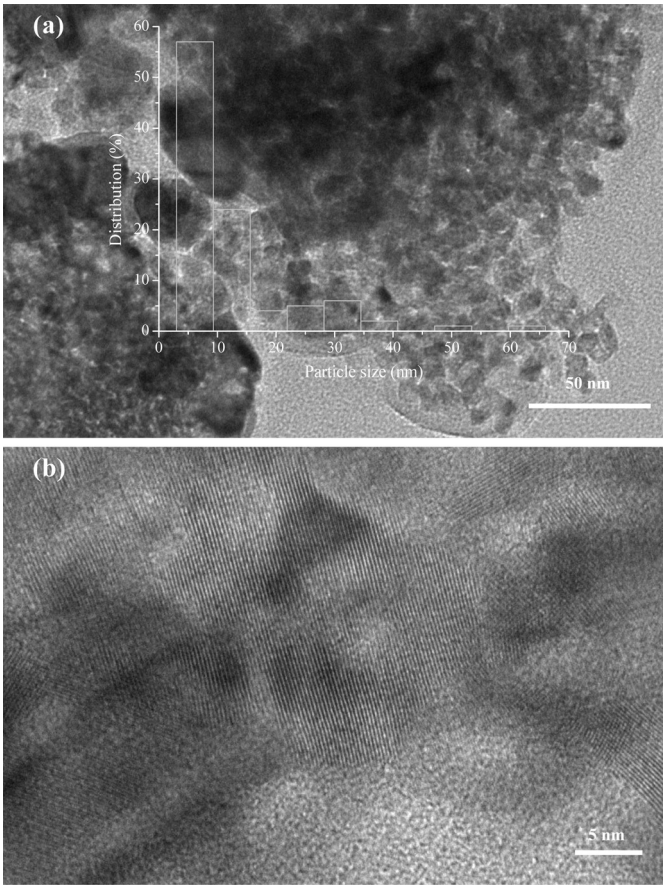

Figure 4. a) TEM and b) high-resolution (HR) TEM images of H_2-reduced Ni_2Zr_8 catalyst.

Conversion of EL into GVL

Initial experiments on the synthesis of GVL from EL in 2-propanol catalyzed by different mixed metal oxides were performed at 230 °C for 0.5 h. As observed in Figure 5, a moderate yield of GVL (65.5%) from EL (79.5% conversion) at a GVL formation rate of 39.4 $mmol\,g^{-1}\,h^{-1}$ was achieved over ZrO_2. The catalytic activity was further improved after introducing an additional metal oxide (e.g., CuO, ZnO, Al_2O_3, Fe_2O_3, and NiO) in combination with ZrO_2, as a result of increased acidity. In particular, the

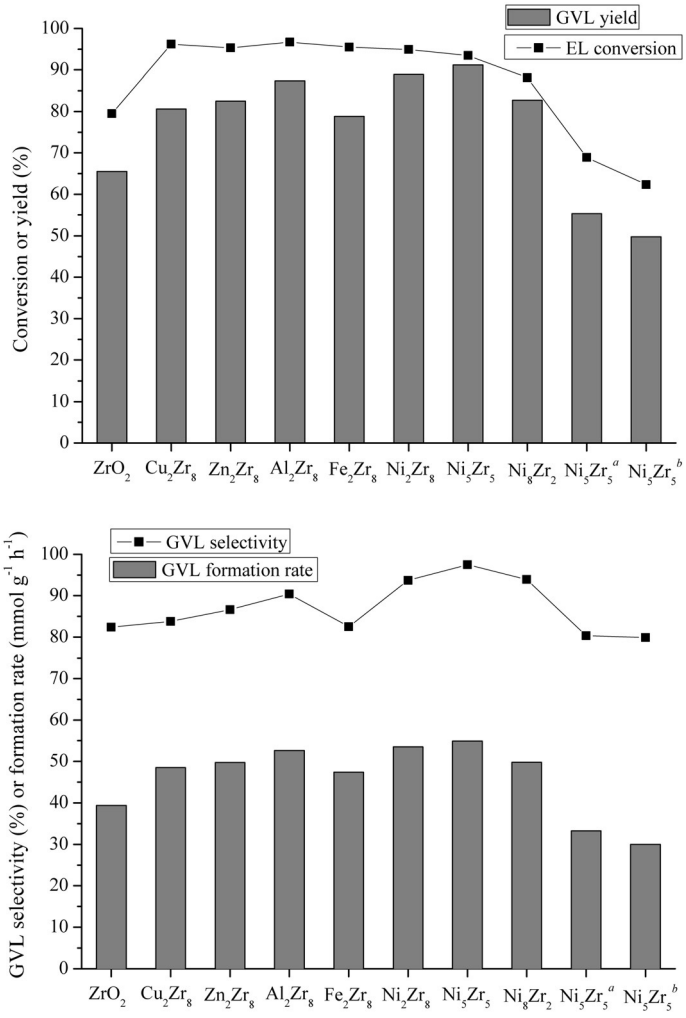

Figure 5. Catalytic conversion of EL into GVL in 2-propanol over mixed metal oxides (EL (0.65 g, 5.5 wt%), 2-propanol (11.8 g), catalyst (0.15 g), at 230 °C and 0.5 h). a) Ni_5Zr_5 was treated with tetraethoxysilane (0.1 g) to cover the Lewis acid sites;[27a] b) Ni_5Zr_5 was titrated with benzoic acid (0.1 g) to poison the Lewis base sites.[27b]

Ni_5Zr_5 catalyst exhibits the highest GVL yield (91.2%), selectivity (97.5%), and formation rate (54.9 mmol g^{-1} h^{-1}), possibly owing to its moderate pore size (5.5 nm), surface area (147.2 m^2 g^{-1}), and acid/base contents (0.72/0.53 mmol g^{-1}), compared with its counterparts Ni_2Zr_8 and Ni_8Zr_2 (Table 1). Moreover, poisoning either the Lewis acid or base sites of the Ni_5Zr_5 catalyst[27] results in a significant decrease in its catalytic performance, which indicates that Lewis acid and base sites appear to play a synergic role in Meerwein–Ponndorf–Verley or CTH reduction,[28] as well as subsequent lactonization to boost the catalytic transformation of EL into GVL.

Effect of reaction temperature and time on EL-to-GVL conversion in ethanol

Based on the above experiments, Ni_5Zr_5 was used as a catalyst to study the influence of temperature and time on the production of GVL from EL (Figure 6). At 230 °C, a high GVL selectivity (97.5%) is obtained in a short time of 0.5 h (Figure 6a). By prolonging the reaction time to 1 h, a slight increase in GVL yield from 91.2 to 92.6% is observed, whereas the selectivity towards GVL decreases to 95.4%. As the reaction time reaches 2 h, both the GVL yield and selectivity decrease, owing to the formation of polymeric compounds (**PC1**–**4**, 2% yield; identified by GC-MS in Figure 8S in the Supporting Information) derived from either GVL or EL (Scheme 1S in the Supporting Information, pathways 1 and 2).[21d] The continuous decrease in GVL yield to 85.8% after 5 h proves that high temperatures are prone to result in the degradation of GVL through condensation reactions (7% yield of condensed products). However, no detectable ring-opening products of GVL or valerate were observed in the reaction mixtures; this may be attributed to the lack of strong Brønsted acid sites provided by zeolites[29] or residual aqueous acids[21e] for GVL ring opening or deoxygenation (removal of hydroxyl groups). At 200 °C (Figure 6b), the highest GVL selectivity of 97.8%, along with a yield of 93.8%, was achieved after 3 h. Interestingly, a certain amount of IPL (3.2–17.7% yield) was detected in a short reaction time of 0.5–2 h; this demonstrates that the key intermediate towards GVL is most likely to be IPL, despite intermediate compounds (ICs), such as isopropyl and ethyl 4-isopropoxypentanoate, also being identified by GC-MS in trace amounts (Scheme 1S, pathway 3, and Figure 8S in the Supporting Information).[21d] More IPL (up to 38.7% yield) is formed at a low temperature of 170 °C (Figure 6c), which supports the reaction pathway 3 illustrated in Scheme 1S in the Supporting Information. However, it is almost impossible to avoid side reactions (< 10% yields), which lead to a decrease in GVL yield and selectivity at even lower temperatures (e.g., 170 and 200 °C). On the contrary, a much longer time is required to obtain high yields of GVL.

Direct conversion of sugars into GVL

The one-pot synthesis of GVL directly from biomass-derived carbohydrates, including fructose, glucose, cellobiose, and carboxymethyl cellulose, was subsequently examined, and all experiments were performed in an alcoholic solvent at 200 °C. In Table 2, both Ni_5Zr_5 oxide and H_2-reduced Ni_5Zr_5 catalyzed the conversion of EL into GVL in high yields, as determined by GC (93.8 and 95.2%, respectively; Table 2, entries 1 and 2), as well as those isolated (88.2 and 91.9%, respectively; ^1H and ^{13}C NMR spectra provided in Figure 9S in the Supporting Information) by column chromatography (ethyl acetate/hexane = 1:5). Apart from GVL yields, the mass balance and GVL formation rates of NiZr samples are also superior to previously reported catalytic systems (Table 2, entries 3–8). Both of them are almost inactive for the synthesis of GVL from fructose after 3 h, except for a small amount of IPL generated (Table 2, entries 9 and 10). Instead of 2-propanol, ethanol as a solvent and hydrogen donor is able to somehow improve the conversion

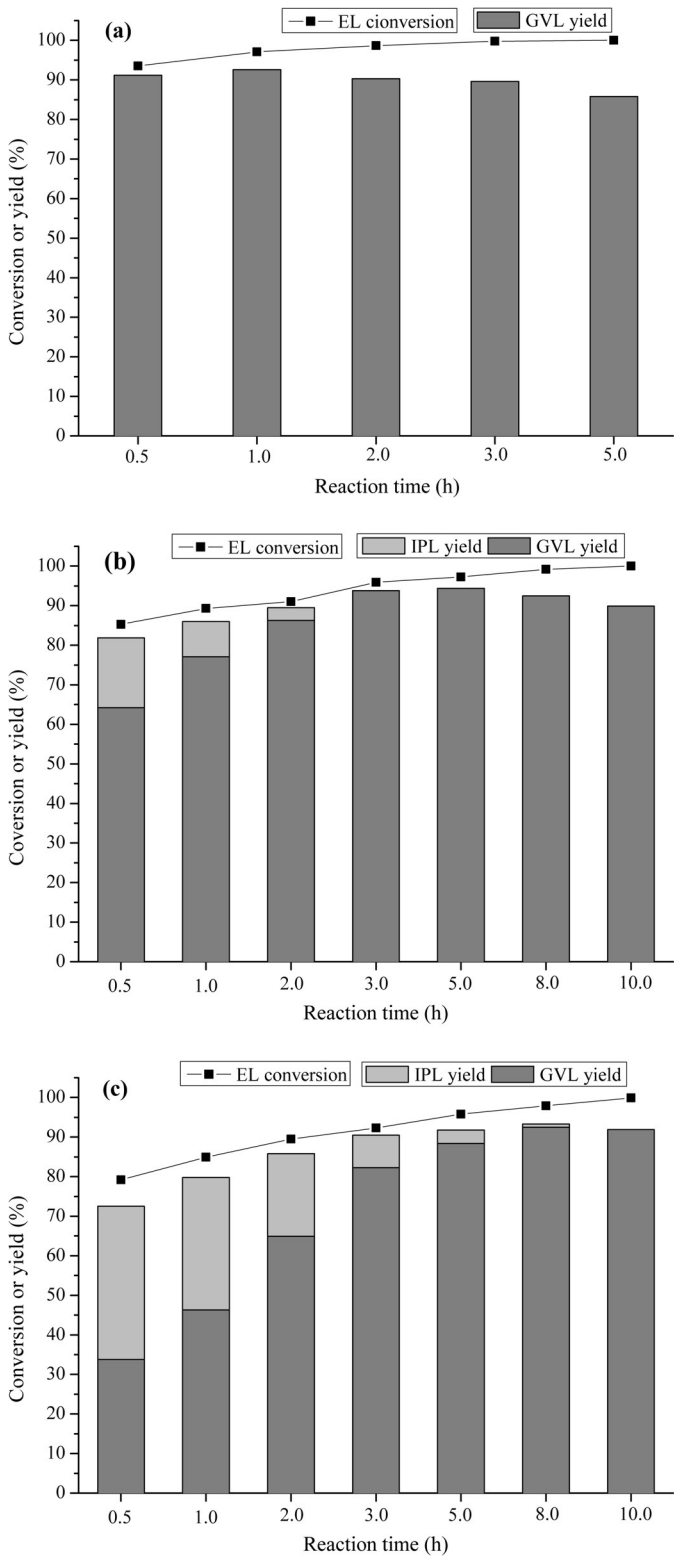

Figure 6. Catalytic conversion of EL into GVL in 2-propanol over the Ni_5Zr_5 catalyst at a) 230, b) 200, and c) 170 °C by varying the reaction time (EL (0.65 g, 5.5 wt%), 2-propanol (11.8 g), and Ni_5Zr_5 (0.15 g)). IPL = isopropyl levulinate.

rate of fructose (53.5%), giving EL in a moderate yield of 31.3% (Table 2, entry 11). The slightly decreased yield of GVL is ascribed to the relatively higher reduction potential of a primary alcohol than that of a secondary alcohol.[30] The introduction of a solid acid, HY6, can significantly increase fructose conversion (88.6%) and the GVL formation rate (2.46 mmol g^{-1} h^{-1}), and promote the formation of EL and GVL in a total yield of 69.5% (Table 2, entry 12). With extension of the reaction from 3 to 7 h, the yield of GVL gradually increases with the consumption of in situ generated EL from fructose (Table 2, entries 12–14). Interestingly, this catalytic system can also mediate the one-pot transformation of glucose, cellobiose, and carboxymethyl cellulose to afford GVL and EL in total yields of 60.1, 56.0, and 51.5%, respectively (Table 2, entries 15–17), with a moderate mass balance (≈70%), which shows great potential for the industrial production of the liquid fuel component of GVL from biomass.

Catalyst cycles

Ni_5Zr_5 oxide and its counterpart magnetic nanocatalyst (H_2-reduced Ni_5Zr_5) were recycled for the conversion of EL into GVL in 2-propanol at 200 °C for 3 h (Figure 7). Both catalysts tolerate the reaction conditions, and exhibit almost constant activity in 3 or 5 consecutive cycles, with slightly decreasing GVL yield from 93.8 to 86.5%, and 95.2 to 90.9%, respectively. To examine the leachability of the H_2-reduced Ni_5Zr_5 catalyst, the magnetic sample was separated from the reaction mixture after 0.5 h and the rest of the alcoholic solution was further reacted for another 0.5 h without adding any catalyst. No significant difference in terms of EL conversion (89.3% vs. 90.9%) and GVL yield (72.4% vs. 72.2%) was observed; moreover, only 0.3 wt% Ni and 0.5% Zr leached into 2-propanol, as detected by ICP-OES, which implies the heterogeneous nature of the catalyst. Furthermore, the XRD patterns and CO_2-TPD profiles of fresh and reused (in the fifth cycle) magnetic nanocatalysts were also investigated (Figures 10S and 11S in the Supporting Information), and the unchanged structure and slight increase in base density possibly resulted from the adsorption of organ-

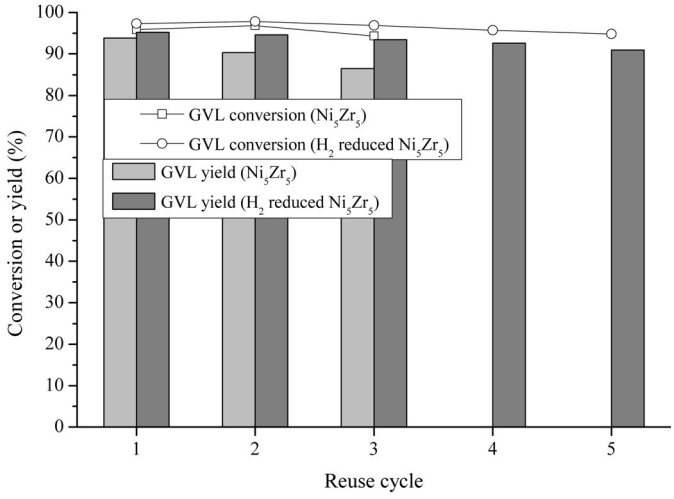

Figure 7. Recycling of Ni_5Zr_5 and H_2-reduced Ni_5Zr_5 catalysts for the EL-to-GVL conversion in 2-propanol (EL (0.65 g, 5.5 wt%), 2-propanol (11.8 g), catalyst (0.15 g), 200 °C and 3 h).

Table 2. Direct conversion of biomass derivatives to GVL with H_2-reduced Zr_5Ni_5, HY6, and other catalysts.[a]

Entry	Catalyst	T [°C], t [h]	Substrate	H-donor	Substrate conv. [%]	GVL yield [%]	GVL formation rate [mmol g^{-1} h^{-1}]	Ester (ether) yield [%][c]	Mass balance [%]	Ref.
1	Ni_5Zr_5	200, 3	EL	2-propanol	95.9	93.8 (88.2)[b]	9.41	0	97.9	this study
2	H_2-reduced Ni_5Zr_5	200, 3	EL	2-propanol	97.2	95.2 (91.9)[b]	9.55	0	98.0	this study
3	nano-copper	240, 4	methyl levulinate	methanol	94.1	68.9	2.30	–	74.8	[21e]
4	ZrO_2	150, 16	butyl levulinate	2-butanol	>99.9	84.7	0.98	–	84.8	[21c]
5	$ZrO(OH)_2{\cdot}xH_2O$	200, 1	EL	2-propanol	93.6	88.5	12.3	–	94.9	[21d]
6	Au/ZrO_2	170, 6	butyl levulinate	butyl formate	98	95	<3.17	–	97	[19b]
7	Cu/γ-Al_2O_3	265, 10 min	LA	H_2	98	87	–	–	89	[14b]
8	Cu–Cr	200, 10	LA	H_2	97.8	90.7	8.04	–	92.9	[31]
9	Ni_5Zr_5	200, 3	fructose	2-propanol	36.4	3.2	0.26	17.3	84.1	this study
10	H_2-reduced Ni_5Zr_5	200, 3	fructose	2-propanol	32.6	6.7	0.54	16.5	90.6	this study
11	H_2-reduced Ni_5Zr_5	200, 3	fructose	ethanol	53.5	5.9	0.47	31.3 (2.1)	85.8	this study
12	HY6 + H_2-reduced Ni_5Zr_5[d]	200, 3	fructose	ethanol	88.6	30.7	2.46	38.8 (4.3)	85.2	this study
13	HY6 + H_2-reduced Ni_5Zr_5[d]	200, 5	fructose	ethanol	99.8	43.2	2.08	21.6 (8.9)	73.9	this study
14	HY6 + H_2-reduced Ni_5Zr_5[d]	200, 7	fructose	ethanol	100	48.9	1.68	12.5 (3.2)	64.6	this study
15	HY6 + H_2-reduced Ni_5Zr_5[d]	200, 5	glucose	ethanol	98.3	41.7	2.01	18.4 (11.5)	72.3	this study
16	HY6 + H_2-reduced Ni_5Zr_5[d]	200, 5	cellobiose	ethanol	99.8	35.8	1.81	20.2 (13.4)	69.6	this study
17	HY6 + H_2-reduced Ni_5Zr_5[d]	200, 5	carboxymethyl cellulose	ethanol	–	29.9	1.07	21.6 (15.6)	67.1	this study

[a] Reaction conditions: substrate (0.65 g, 5.5 wt%), ethanol (11.8 g), catalyst (0.15 g) at 200 °C. [b] Yield of GVL isolated is given in parentheses. [c] Ester is denoted as IPL or EL, whereas ether refers to alkyl (isopropyl or ethyl) fructoside or glucoside. [d] H_2-reduced Ni_5Zr_5 (0.10 g) and HY6 (0.05 g) were used as cocatalysts.

ic species (e.g., ethoxides) onto the catalyst surface;[32] this indicates the high stability of H_2-reduced Ni_5Zr_5. For the magnetic catalyst, after NiO was reduced to Ni, the slightly increased activity and stability could be ascribed to the promotion effect of Ni^0 in the process of MPV reduction and the formation of a crystalline structure.

Conclusion

NiZr oxides and their partially reduced counterparts were efficient for GVL production. Hydrogen-reduced magnetic Ni_5Zr_5 was highly active for converting EL into GVL with a high yield of 95.2% at 200 °C after 3 h. More importantly, this magnetic nanocatalyst was easily recovered for 5 cycles with slightly decreasing GVL yield from 95.2 to 90.9%. Furthermore, the combination of the nanocatalyst with a solid acid, HY6, could catalyze the one-pot transformation of fructose, glucose, cellobiose, and carboxymethyl cellulose into GVL and EL in total yields of 69.5, 60.1, 56.0, and 51.5%, respectively.

Experimental Section

Materials

Chemical reagents $Ni(NO_3)_2{\cdot}6H_2O$ (99.99%), $ZrOCl_2{\cdot}8H_2O$ (98.0%), NH_4OH (25–28% in water), and carboxymethyl cellulose (USP) were purchased from Aladdin Industrial Inc. (Shanghai). Ethanol (≥99.5%), 2-propanol (≥99.5%), glucose (≥99.5%), fructose (≥99.0%), and cellobiose (≥99.0%) were purchased from Sigma–Aldrich (Shanghai). GVL (98.0%) and EL (99.0%) were purchased from J&K Scientific Ltd. (Beijing). Other chemicals were of analytical grade and used as received, unless otherwise noted.

Preparation of NiZr catalysts

Acid–base bifunctional NiZr nanocatalysts with Ni/Zr molar ratios of 2/8, 5/5, and 8/2 (denoted as Ni_2Zr_8, Ni_5Zr_5, and Ni_8Zr_2, respectively) were prepared by coprecipitation. In a typical procedure, $Ni(NO_3)_2{\cdot}6H_2O$ (0.58 g, 2 mmol) and $ZrOCl_2{\cdot}8H_2O$ (2.58 g, 8 mmol) were added to deionized water (30 mL) and stirred at room temperature to form a homogeneous mixture, and NH_4OH was injected into the solution by means of a syringe to reach pH 9. The resulting precipitant solution was stirred for 1 h and aged for another 2 h under ambient conditions, followed by filtration (0.22 μm pore size) and washing with water 5 times. The obtained slurry was dried overnight at 80 °C in an oven (WFO-710, EYELA, Tokyo Rikakikai Co., Ltd.), placed into a tubular furnace (SGL-1100, Shanghai Daheng Optics and Fine Mechanics Co., Ltd.), and heated to 450 °C at a heating rate of 2 °C min^{-1} for 3 h of calcination in air. For comparison, Cu_2Zr_8, Zn_2Zr_8, Al_2Zr_8, and Fe_2Zr_8 were also prepared by using the same synthetic method as that described above. On the other hand, to facilitate the process of catalyst separation, the calcined NiZr oxide samples with Ni/Zr molar ratios of 2:8, 5:5, and 8:2 were further reduced in the tubular furnace under a flow of H_2 (1 vol% in N_2) at 550 °C (with a heating rate of 2 °C min^{-1}) for 3 h, and the resulting catalysts were designated as H_2-reduced Ni_2Zr_8, Ni_5Zr_5, and Ni_8Zr_2, respectively. All samples were ground and passed through 200 mesh sieves before use in experiments.

Catalyst characterization

XRD patterns were recorded with a D/max-TTR III X-ray powder diffractometer (Rigaku International Corp., Tokyo) by using a $Cu_{K\alpha}$ ra-

diation source. XPS measurements were performed by using a Physical Electronics Quantum 2000 Scanning ESCA Microprobe (Physical Electronics Inc., PHI, MN) equipped with a monochromatic $Al_{K\alpha}$ anode. The elemental compositions of the catalysts, after being dissolved in water with concentrated acid, were determined by ICP-OES on an Optima 5300 DV instrument (PerkinElmer Inc., Waltham, MA). BET surface areas of the porous materials were determined from nitrogen physisorption measurements at liquid nitrogen temperature on a Micromeritics ASAP 2010 instrument (Tristar II 3020, Norcross, GA). NH_3- and CO_2-TPD analyses were conducted on an automated chemisorption analyzer (Quantachrome Instruments, Boynton Beach, FL) to assess the surface acidity and basicity of catalysts, respectively. The magnetic properties of powder catalysts were measured by means of VSM (HH-15, Nanda Instrument Plant, Nanjing) at room temperature. Magnified images of samples were obtained with a transmission electron microscope (TEM; JEM-1200EX, JEOL, Tokyo), and the size distribution of selected catalysts were estimated from the TEM images by using Nano Measurer 1.2 software to give the corresponding mean particle diameters.

Catalytic conversion of sugars and EL into GVL

The production of GVL from sugar or EL was performed in a 25 mL stainless-steel autoclave (YZPR-25, YanZheng Shanghai Experimental Instrument Co., Ltd.) with dead volume (0.5 mL; pressure gauge was removed). In a typical procedure, catalyst (0.15 g) was added to a stock solution consisting of substrate (0.65 g, 5.5 wt%, relative to alcohol) and alcohol (11.8 g). The autoclave was flushed with nitrogen 3 times before being heated to the desired temperature (i.e., 170, 200, and 230 °C) within 50 min. The air-free reactant mixture was magnetically stirred at 500 rpm for a specific reaction time (0.5–10 h), and time zero was defined as the designated temperature reached. After the reaction, the autoclave was quenched in a water bath. The reaction mixture was directly decanted from the Teflon liner, from which the magnetic catalyst was attracted by a permanent magnet. The remaining catalyst in the liner was washed with ethanol 3 times, dried at 80 °C for 2 h (catalyst recovery rate of 89–93%), and directly used in the next cycles. For catalysts without magnetism, centrifugation was employed to separate them from solutions.

Analysis of products

Liquid products and byproducts were identified by GC-MS (Agilent 6890N GC/5973 MS, Santa Clara, CA). The concentrations of fructose, glucose, and cellobiose in alcoholic solution (after dilution 10 times with deionized water) were determined by HPLC (LC-20A, Shimadzu, Kyoto) fitted with an Aminex HPX-87H column (Bio-Rad, Richmond, CA) and a refractive index (RI) detector as well as a UV detector at $\lambda = 280$ nm. EL, GVL, and IPL were analyzed by GC (GC-2014, Shimadzu, Kyoto) with an Rtx-Wax capillary column (30 m × Ø0.25 mm × 0.25 μm) and a flame ionization detector. N_2 was used as the carrier gas at a flow rate of 0.75 mL min^{-1}, and a programmed temperature of 60 °C (1 min)–10 °C min^{-1}–230 °C (5 min) was employed in the analysis. An internal standard (*n*-butylalcohol) was used for quantitative analysis, and EL conversion and GVL yield were calculated on the basis of the standard curves made from commercial samples. EL or sugar conversion (*X*, mol%) and GVL yield (*Y*, mol%) were calculated by using Equations (1) and (2):

$$X(\%) = \frac{1-(\text{mole of EL or sugar in products})}{(\text{mole of initial EL or sugar})} \times 100\,\% \qquad (1)$$

$$Y(\%) = \frac{\text{mole of GVL}}{\text{mole of initial EL or sugar monomers}} \times 100\,\% \qquad (2)$$

Acknowledgements

We acknowledge financial support from the Chinese Academy of Sciences (CAS 135 program (XTBG-T02) and equipment R&D grant (no. YZ201260)), the Yunnan Provincial Government (Baiming Haiwai Gaocengci Rencai Jihua), and the Natural Science Foundation of China (no. 21576059).

Keywords: biomass · heterogeneous catalysis · magnetic properties · metal oxides · nanoparticles

[1] a) C. Xu, R. A. D. Arancon, J. Labidi, R. Luque, *Chem. Soc. Rev.* **2014**, *43*, 7485–7500; b) S. Dutta, S. De, B. Saha, *ChemPlusChem* **2012**, *77*, 259–272; c) Y. Zhang, Y. Chen, Y. Shen, Y. Yan, J. Pan, W. Shi, L. Yu, *ChemPlusChem* **2015**, DOI: 10.1002/cplu.201500357; d) H. Li, P. S. Bhadury, A. Riisager, S. Yang, *Catal. Sci. Technol.* **2014**, *4*, 4138–4168; e) R. Liu, J. Chen, L. Chen, Y. Guo, J. Zhong, *ChemPlusChem* **2014**, *79*, 1448–1454; f) Z. Zhang, Y. Wang, Z. Fang, B. Liu, *ChemPlusChem* **2014**, *79*, 233–240; g) A. Chen, Y. Li, J. Chen, G. Zhao, L. Ma, Y. Yu, *ChemPlusChem* **2013**, *78*, 1370–1378; h) H. Li, S. Saravanamurugan, S. Yang, A. Riisager, *Green Chem.* **2015**, DOI: 10.1039/c5gc01043h; i) C. Wang, F. Yuan, L. Liu, X. Niu, Y. Zhu, *ChemPlusChem* **2015**, 11, 1657–1665.

[2] a) J. S. Luterbacher, J. M. Rand, D. M. Alonso, J. Han, J. T. Youngquist, C. T. Maravelias, B. F. Pfleger, J. A. Dumesic, *Science* **2014**, *343*, 277–280; b) L. Zhang, H. Yu, P. Wang, Y. Li, *Bioresour. Technol.* **2014**, *151*, 355–360; c) L. Qi, I. T. Horváth, *ACS Catal.* **2012**, *2*, 2247–2249; d) L. Qi, Y. F. Mui, S. W. Lo, M. Y. Lui, G. R. Akien, I. T. Horváth, *ACS Catal.* **2014**, *4*, 1470–1477; e) G. Strappaveccia, L. Luciani, E. Bartollini, A. Marrocchi, F. Pizzo, L. Vaccaro, *Green Chem.* **2015**, *17*, 1071–1076; f) G. Strappaveccia, E. Ismalaj, C. Petrucci, D. Lanari, A. Marrocchi, M. Drees, A. Facchetti, L. Vaccaro, *Green Chem.* **2015**, *17*, 365–372; g) E. Ismalaj, G. Strappaveccia, E. Ballerini, F. Elisei, O. Piermatti, D. Gelman, L. Vaccaro, *ACS Sustainable Chem. Eng.* **2014**, *2*, 2461–2464; h) P. Pongrácz, L. Kollár, L. T. Mika, *Green Chem.* **2015**, DOI: 10.1039/C5GC01778E; i) V. Fábos, M. Y. Lui, Y. F. Mui, Y. Y. Wong, L. T. Mika, L. Qi, E. Cséfalvay, V. Kovács, T. Szűcs, I. T. Horváth, *ACS Sustainable Chem. Eng.* **2015**, *3*, 1899–1904.

[3] a) I. T. Horváth, H. Mehdi, V. Fábos, L. Boda, L. T. Mika, *Green Chem.* **2008**, *10*, 238–242; b) D. M. Alonso, S. G. Wettstein, J. A. Dumesic, *Green Chem.* **2013**, *15*, 584–595.

[4] a) H. Mehdi, V. Fábos, R. Tuba, A. Bodor, L. T. Mika, I. T. Horváth, *Top. Catal.* **2008**, *48*, 49–54; b) K. Yan, Y. Yang, J. Chai, Y. Lu, *Appl Catal. B: Environ.* **2015**, *179*, 292–304; c) F. Geilen, B. Engendahl, A. Harwardt, W. Marquardt, J. Klankermayer, W. Leitner, *Angew. Chem. Int. Ed.* **2010**, *49*, 5510–5514; *Angew. Chem.* **2010**, *122*, 5642–5646; d) F. M. Geilen, B. Engendahl, M. Hölscher, J. Klankermayer, W. Leitner, *J. Am. Chem. Soc.* **2011**, *133*, 14349–14358.

[5] a) D. Fegyverneki, L. Orha, G. Láng, I. T. Horváth, *Tetrahedron* **2010**, *66*, 1078–1081; b) A, Strádi, M. Molnár, M. Óvári, G. Dibó, F. U. Richter, L. T. Mika, *Green Chem.* **2013**, *15*, 1857–1862; c) A. Strádi, M. Molnár, P. Szakál, G. Dibó, D. Gáspár, L. T. Mika, *RSC Adv.* **2015**, *5*, 72529–72535.

[6] a) M. Chalid, H. J. Heeres, A. A. Broekhuis, *J. Appl. Polym. Sci.* **2012**, *123*, 3556–3564; b) P. K. Wong, C. Li, L. Stubbs, Patent Appl. WO 2012/134397A1, **2012**.

[7] a) K. Yan, C. Jarvis, J. Gu, Y. Yan, *Renewable Sustainable Energy Rev.* **2015**, *51*, 986–997; b) J. M. Tukacs, B. Fridrich, G. Dibó, E. Székely, L. T. Mika, *Green Chem.* **2015**, DOI: 10.1039/C5GC01099C.

[8] X. Tang, X. Zeng, Z. Li, L. Hu, Y. Sun, S. Liu, T. Lei, L. Lin, *Renewable Sustainable Energy Rev.* **2014**, *40*, 608–620.

[9] a) K. Osakada, T. Ikariya, S. Yoshikawa, *J. Organomet. Chem.* **1982**, *231*, 79 – 90; b) J. M. Tukacs, D. Király, A. Strádi, G. Novodarszki, Z. Eke, G. Dibó, T. Kégl, L. T. Mika, *Green Chem.* **2012**, *14*, 2057 – 2065; c) J. M. Tukacs, M. Novák, G. Dibó, L. T. Mika, *Catal. Sci. Technol.* **2014**, *4*, 2908 – 2912.

[10] a) W. R. Wright, R. Palkovits, *ChemSusChem* **2012**, *5*, 1657 – 1667; b) W. Luo, M. Sankar, A. M. Beale, Q. He, C. J. Kiely, P. C. A. Bruijnincx, B. M. Weckhuysen, *Nat. Commun.* **2015**, *6*, 6540.

[11] J. M. Tukacs, R. V. Jones, F. Darvas, G. Dibó, G. Lezsák, L. T. Mika, *RSC Adv.* **2013**, *3*, 16283 – 16287.

[12] a) C. Moreno-Marrodan, P. Barbaro, *Green Chem.* **2014**, *16*, 3434 – 3438; b) A. Villa, M. Schiavoni, C. E. Chan-Thaw, P. F. Fulvio, R. T. Mayes, S. Dai, K. L. More, G. M. Veith, L. Prati, *ChemSusChem* **2015**, *8*, 2520 – 2528.

[13] O. A. Abdelrahman, A. Heyden, J. Q. Bond, *ACS Catal.* **2014**, *4*, 1171 – 1181.

[14] a) V. Mohan, V. Venkateshwarlu, C. V. Pramod, B. D. Raju, K. S. R. Rao, *Catal. Sci. Technol.* **2014**, *4*, 1253 – 1259; b) B. Putrakumar, N. Nagaraju, V. P. Kumar, K. V. R. Chary, *Catal. Today* **2015**, *250*, 209 – 217.

[15] a) K. Shimizu, S. Kanno, K. Kon, *Green Chem.* **2014**, *16*, 3899 – 3903; b) H. Zhou, J. Song, H. Fan, B. Zhang, Y. Yang, J. Hu, Q. Zhu, B. Han, *Green Chem.* **2014**, *16*, 3870 – 3875.

[16] L. Deng, J. Li, D.-M. Lai, Y. Fu, Q. X. Guo, *Angew. Chem. Int. Ed.* **2009**, *48*, 6529 – 6532; *Angew. Chem.* **2009**, *121*, 6651 – 6654.

[17] C. Ortiz-Cervantes, M. Flores-Alamo, J. J. García, *ACS Catal.* **2015**, *5*, 1424 – 1431.

[18] V. Fábos, L. T. Mika, I. T. Horváth, *Organometallics* **2014**, *33*, 181 – 187.

[19] a) L. Deng, Y. Zhao, J. Li, Y. Fu, B. Liao, Q.-X. Guo, *ChemSusChem* **2010**, *3*, 1172 – 1175; b) X. L. Du, Q. Y. Bi, Y. M. Liu, Y. Cao, K. N. Fan, *ChemSusChem* **2011**, *4*, 1838 – 1843; c) J. Yuan, S. S. Li, L. Yu, Y. M. Liu, Y. Cao, H. Y. He, K. N. Fan, *Energy Environ. Sci.* **2013**, *6*, 3308 – 3313.

[20] A. Boddien, D. Mellmann, F. Gärtner, R. Jackstell, H. Junge, P. J. Dyson, G. Laurenczy, R. Ludwig, M. Beller, *Science* **2011**, *333*, 1733 – 1736.

[21] a) Z. Yang, Y. B. Huang, Q. X. Guo, Y. Fu, *Chem. Commun.* **2013**, *49*, 5328 – 5330; b) J. Geboers, X. Wang, A. B. de Carvalho, R. Rinaldi, *J. Mol. Catal. A: Chem.* **2014**, *388 – 389*, 106 – 115; c) M. Chia, J. A. Dumesic, *Chem. Commun.* **2011**, *47*, 12233 – 12235; d) X. Tang, H. Chen, L. Hu, W. Hao, Y. Sun, X. Zeng, L. Lin, S. Liu, *Appl. Catal. B* **2014**, *147*, 827 – 834; e) X. Tang, Z. Li, X. Zeng, Y. Jiang, S. Liu, T. Lei, Y. Sun, L. Lin, *ChemSusChem* **2015**, *8*, 1601 – 1607.

[22] H. Y. Luo, D. F. Consoli, W. R. Gunther, Y. Román-Leshkov, *J. Catal.* **2014**, *320*, 198 – 207.

[23] A. S. Amarasekara, M. A. Hasan, *Catal. Commun.* **2015**, *60*, 5 – 7.

[24] a) J. Song, B. Zhou, H. Zhou, L. Wu, Q. Meng, Z. Liu, B. Han, *Angew. Chem.* **2015**, *127*, 9531 – 95235; b) J. Song, L. Wu, B. Zhou, H. Zhou, H. Fan, Y. Yang, Q. Meng, B. Han, *Green Chem.* **2015**, *17*, 1626 – 1632.

[25] a) G. R. Akien, L. Qi, I. T. Horváth, *Chem. Commun.* **2012**, *48*, 5850 – 5852; b) G. Novodárszki, N. Rétfalvi, G. Dibó, P. Mizsey, E. Cséfalvay, L. T. Mika, *RSC Adv.* **2014**, *4*, 2081 – 2088.

[26] F. Liguori, C. Moreno-Marrodan, P. Barbaro, *ACS Catal.* **2015**, *5*, 1882 – 1894.

[27] a) V. V. Ordomsky, V. L. Sushkevich, J. C. Schouten, J. van der Schaaf, T. A. Nijhuis, *J. Catal.* **2013**, *300*, 37 – 46; b) F. M. Bautista, J. M. Campelo, A. García, D. Luna, J. M. Marinas, R. A. Quirós, A. A. Romero, *Appl. Catal. A* **2003**, *243*, 93 – 107.

[28] P. S. Kumbhar, J. Sanchez-Valente, J. Lopez, F. Figueras, *Chem. Commun.* **1998**, 535 – 536.

[29] J.-P. Lange, R. Price, P. M. Ayoub, J. Louis, L. Petrus, L. Clarke, H. Gosselink, *Angew. Chem. Int. Ed.* **2010**, *49*, 4479 – 4483; *Angew. Chem.* **2010**, *122*, 4581 – 4585.

[30] J. C. Van der Waal, P. J. Kunkeler, K. Tan, H. Van Bekkum, *J. Catal.* **1998**, *173*, 74 – 83.

[31] K. Yan, A. Chen, *Energy* **2013**, *58*, 357 – 363.

[32] V. L. Sushkevich, I. I. Ivanova, S. Tolborg, E. Taarning, *J. Catal.* **2014**, *316*, 121 – 129.

Manuscript received: October 28, 2015
Accepted Article published: November 2, 2015
Final Article published: November 19, 2015